

# CFD ANALYSIS OF THE EFFECT OF SELF-REGULATING DEVICES ON THE DISTRIBUTION OF NATURALLY SUPPLIED AIR

J. De Neve<sup>1</sup>, S. Denys<sup>1</sup>, J.G. Pieters<sup>1</sup>, I. Pollet<sup>2</sup> and J. Denul<sup>2</sup>

<sup>1</sup> *Department of Biosystems Engineering, Ghent University, Ghent, B 9000-Belgium*

<sup>2</sup> *Renson Ventilation NV, Waregem, B 8790-Belgium*

## ABSTRACT

Thermal comfort in living rooms or bedrooms is among others determined by the spatial distribution of the supplied ventilation air. In this work, the performance of a self-regulating (pressure-sensitive) air transfer device, in terms of air flow rate and human comfort, was investigated by means of CFD. Self-regulating ventilators limit the air supply rate according to the pressure difference across the ventilator as to reduce draught risks. The CFD analysis was carried out as much as possible according to the experimental method for evaluating such devices, described in the European Standard EN 13141-1. Pressure differences across the air transfer device of 2 and 10 Pa were studied, at a temperature difference between inside and outside climate of 20 °C. Results revealed that self-regulating air transfer devices are able to achieve a uniform flow rate for the pressure differences under investigation. Besides, they decrease the risk on draught compared with non-regulating devices.

## KEYWORDS

Natural ventilation, energy performance of buildings, modelling, computational fluid dynamics, thermal comfort, draught

## INTRODUCTION

Many buildings throughout the world are naturally ventilated. In the past, natural ventilation relied on an arbitrary combination of uncontrolled air infiltration and opening or closing windows and doors. Nowadays, ventilation requirements can be very demanding, as modern systems must provide greatly improved reliability and control. Natural ventilation is driven by wind and thermally generated pressure differences (so-called stack pressures). For a given configuration of openings, the rate of natural ventilation varies according to the prevailing driving forces of wind and indoor/outdoor temperature differences. Therefore, in the design of natural ventilation devices, provision is often made for the occupant to be able to adjust ventilation device openings to meet the demand. Besides user adjustable systems, some air inlet systems respond automatically to climate parameters such as temperature, humidity or pressure. So-called 'pressure-sensitive vents' have been specifically designed for operation at the normal driving pressures of natural ventilation (i.e., < 10 Pa). The aim of designers is to enable an almost uniform flow rate to be achieved throughout a wide pressure range, thus permitting good control of natural ventilation.

For assessing and designing natural ventilation devices, physical models can be very useful. Single-compartment and multi-compartment mass balance models have been designed to estimate the impact of sources, sinks and control options on indoor pollutant concentrations

(e.g., AIVC, 1990; Koontz and Nagda, 1991; Sparks *et al.*, 1996). However, for assessing the performance of natural ventilation devices in terms of flow rate and pressure sensitivity, mass balance models do not provide the desired information. In such cases, models based on computational fluid dynamics (CFD) provide more detailed information. CFD models predict air velocity, temperatures, pressures and pollutant concentrations at individual points in a room instead of the average values predicted by mass balance models. As a result, CFD models are especially useful for studying the distribution of air and air movement in rooms and buildings (Jones and Whittle, 1992; Nielsen, 1996), and for evaluating thermal comfort (Dorer *et al.*, 2005). In this work, ventilation devices placed in the window or outer wall as natural air supply (so-called background ventilators), were studied using CFD. In particular, the performance of a self-regulating (pressure-sensitive) air transfer device, in terms of air flow rate and human comfort feeling, was investigated. The CFD-analysis was carried out as much as possible according to the experimental method for evaluating such devices, described in the European standard EN 13141-1.

## MATERIALS AND METHODS

### Climate room

A CAD design of a climate room was generated as shown in Figure 1. The room had three interior walls and one exterior wall. The exterior wall (thickness 40 cm) had a centrally located window opening of 1.18 m × 1.45 m (H×W). The window opening was positioned at 0.82 m above the floor. Hence, the top of the opening was at 2 m. The window consisted of an exterior and interior frame, an air transfer device with opening length of 1 m and a window glass.

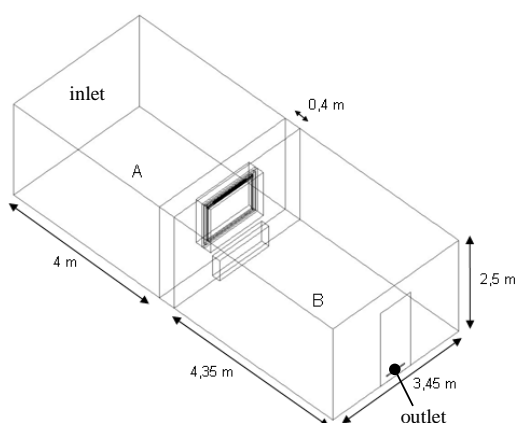


Figure 1: Geometry of the calculation domain with (A) the outdoor environment and (B) the room

The wall opposing the window wall contained a door of 2 m × 0.83 m with an opening of 3 cm × 50 cm (H×W) placed at 15 cm above the floor. This opening served as the outlet of the climate room. A rectangular block (0.55 m × 0.20 m × 1.35 m), placed under the window at a height of 15 cm, served as the heating device.

The investigated air transfer device (Figure 2) was placed on top of the window frame. It had a manually adjustable outlet lid and a self-regulating, pressure-sensitive interior flap (Figure 2). The self-regulating flap was simulated in two positions, corresponding to pressure

differences of 2 and 10 Pa over the air transfer device. The corresponding positions of the flap were experimentally determined.

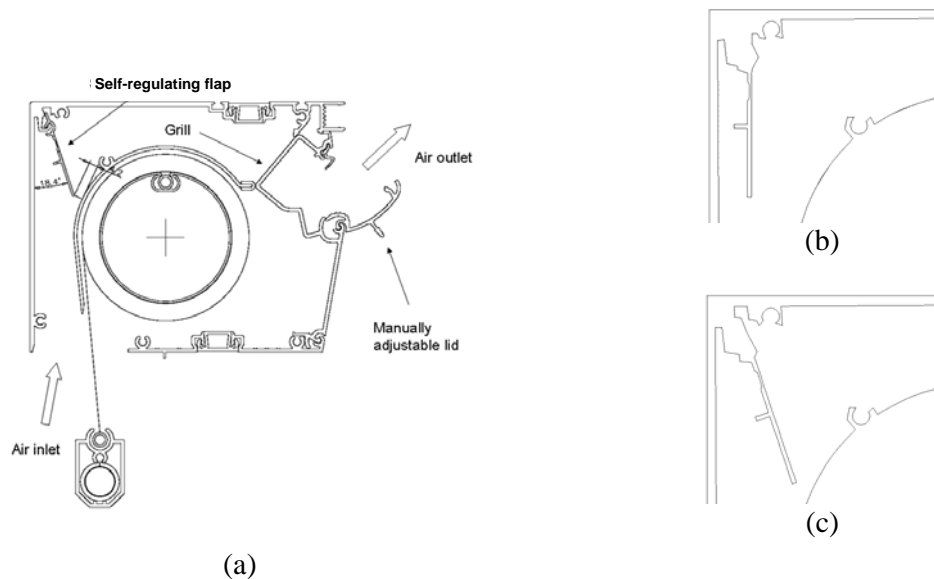


Figure 2: (a) Geometry of the air transfer device with its manually adjustable outlet lid and pressure-sensitive interior flap and a detail of the geometry of the interior flap in its position of (b) 2 Pa and (c) 10 Pa.

## CFD-model and procedures

The CFD analysis was performed using the commercial CFD software Fluent (Fluent Inc., Lebanon, U.S.). This software uses the finite volume method. The segregated solver was used to obtain steady-state solutions. The numerical discretisation was conducted by a first order upwind scheme. Turbulence was simulated by a  $k-\omega$  model, modified for low Reynolds number effects and hence applicable to wall-bounded flows and free shear flows. Natural convection was simulated by including gravity and temperature dependent air densities according to the ideal gas law.

Simulations were done for two positions of the pressure-sensitive interior flap, corresponding to pressure differences of 2 (POS2) and 10 Pa (POS10) over the air transfer device (Figure 2). For these simulations, a relative pressure of 2 or 10 Pa was applied at the inlet of the calculation domain. Besides simulations for corresponding pressure differences and flap positions (simulations POS2-2Pa and POS10-10Pa), a simulation was performed for a non-regulating case whereby a pressure difference of 10 Pa was considered for a flap position corresponding to the design at 2 Pa (POS2-10Pa). The latter simulation was done for evaluating the ability of the air transfer device to achieve a uniform flow rate throughout a wide pressure range.

Except for the inlet face, all other faces of the calculation domain (door, interior walls, floor and the ceiling) were treated as adiabatic walls. The exterior wall, the window frame and the window glass were solids with a thermal conductivity of respectively 0.2 W/(m·K), 0.12 W/(m·K) and 0.065 W/(m·K). The pressure at the outlet was adapted in such a way that the pressure difference over the air transfer device was 2 or 10 Pa. Pressure adaptations were needed to overcome the flow resistance at the outlet (door opening).

The experimental method for evaluating air transfer devices, described in EN 13141-1, imposes a constant temperature in the test room. A central heating-like thermal regulation procedure was therefore incorporated in the model to control the temperature inside the ventilated room. The control procedure adapted the surface temperature of the heating device, during the CFD calculation, so the desired temperature was achieved in the middle of the room. The outdoor temperature was 0 °C and the desired temperature in the middle of the room was set at  $(20 \pm 0.5)$  °C.

## RESULTS AND DISCUSSION

### Air transfer device performance

Results for the three cases are included in Table 1. The self-regulating performance of the air transfer device can be clearly seen: at a pressure difference of 10 Pa, almost the same flow rate was achieved as at a pressure difference of 2 Pa (40.36 m<sup>3</sup>/h and 43.56 m<sup>3</sup>/h, respectively). As a result, similar air patterns were observed in both pressure-regulated cases (see Figure 3a). In the case where the pressure-sensitive interior flap was not positioned according to the prevailing pressure difference (POS2-10Pa), the higher pressure difference resulted in a much higher flow rate of 108.84 m<sup>3</sup>/h. Apparently, the position of the interior flap caused an extra flow resistance at higher pressure differences, decreasing the flow rate.

TABLE 1  
Simulation results of the three cases

Simulation	POS2-2Pa	POS10-10Pa	POS2-10Pa
Position self-regulating device (Pa)	2	10	2
Pressure difference (Pa)	2.02	10.08	10.04
Flow rate (m <sup>3</sup> /h)	43.56	40.36	108.84
Heating device temperature (K)	345	345	377
Heating device capacity (W)	362	329	616
Average draught risk (%)	4.56	5.89	8.87

### Human comfort

High flow rates have a negative influence on the human comfort. Figure 3a shows the velocity contours with isolines of 0.2 m/s, in the vertical plane of symmetry, perpendicular to the window. The higher flow rate in the case POS2-10Pa resulted in an air jet that penetrated horizontally into the room. For the self-regulating cases POS2-2Pa and POS10-10Pa, the velocities at the air transfer device were lower, allowing for a downward movement of the cold and heavy infiltrating air as a result of gravity. Besides velocities, also the temperature distribution in the room contributes to the feeling of comfort (Figure 3b). The air jet, observed in the non-regulating case POS2-10Pa, brought a significant amount of cold air deep into the room, while in the other cases, infiltrating cold air was heated up by the heating device and subsequently distributed within the room, which resulted in better mixing. As a result, a significantly higher heating device capacity was needed to reach the desired room temperature in the case POS2-10Pa (see Table 1). The model approximation of the heating device as a rectangular block with low contact area, and the fact that no radiation was taken into account, gave rise to unrealistically high heating device temperatures, specially in the latter case. In the cases where flow rates were regulated, the required heating device temperature and the

corresponding capacity were lower due to a better contact between cold infiltrating air and the heating device, and better mixing.

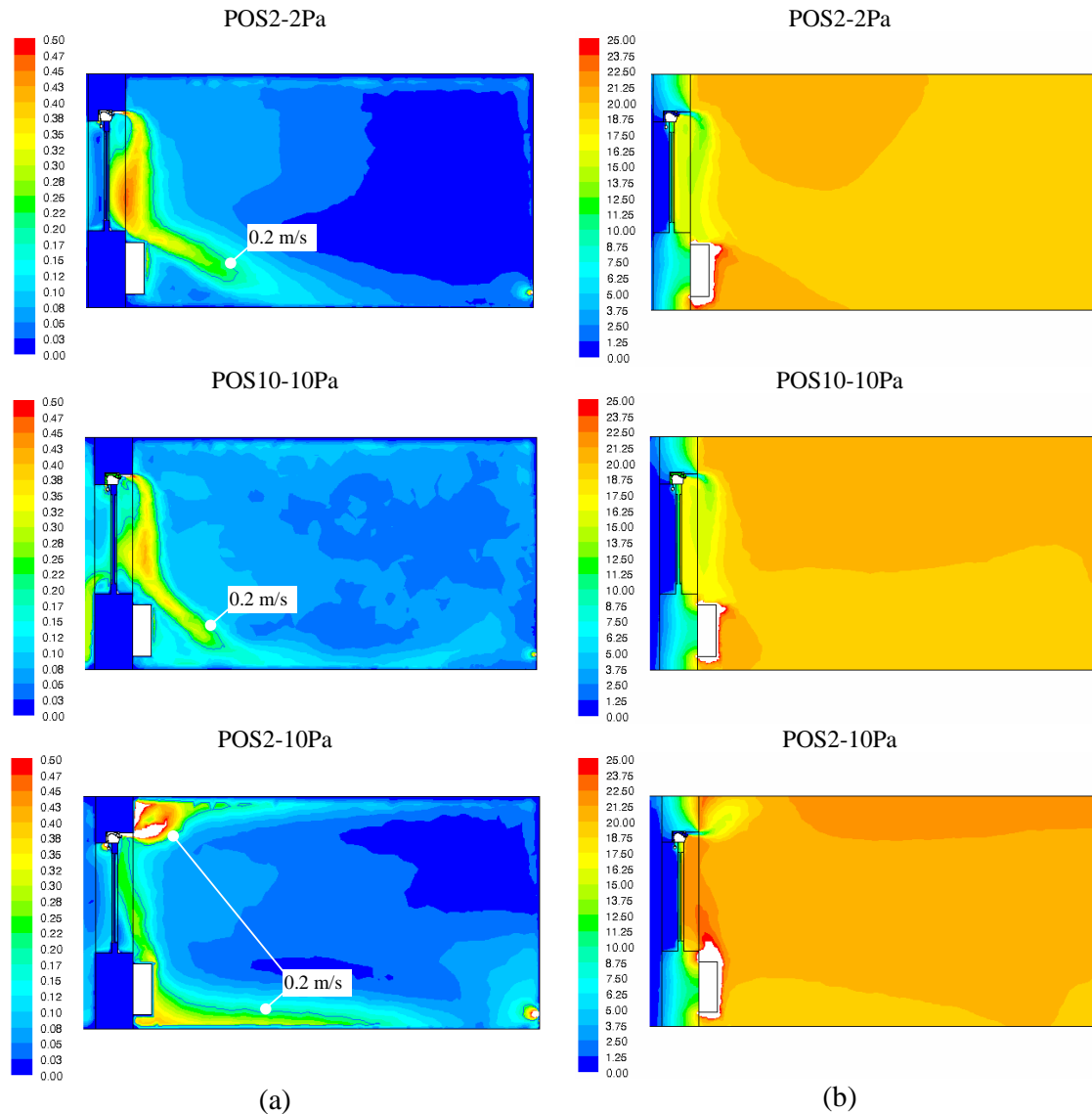


Figure 3: (a) Velocity magnitude (m/s) with isolines of 0.2 m/s and (b) temperature distribution (°C) for POS2-2Pa, POS10-10Pa and the POS2-10Pa

Effects of air velocity and temperature fields on the human comfort feeling can be brought together in the ‘draught rate’. Draught is defined as an undesirable local cooling of the body caused by air movement, and is the most common complaint in relation to indoor climate. ISO 7730 defines draught rate  $DR$  (%) by means of the following equation, used to estimate the percentage of people likely to be dissatisfied because of air movements:

$$DR = (34 - t_a) \times (v_a - 0.05)^{0.6223} \times (0.3693 \times v_a \times TU + 3.143)$$

where  $t_a$  is the air temperature (°C),  $v_a$  the local mean air velocity (m/s) and  $TU$  the turbulence intensity (%). Figure 4 shows profiles of the draught rate on the plane of symmetry for the self-regulating case POS10-10Pa and the non-regulating case POS2-10Pa. Since only one plane is shown, it is difficult to draw conclusions. For comparison, volume-average values of

$DR$  within the room are included in Table 1. The volume-averaged  $DR$  was higher for POS10-10Pa than for POS2-2Pa, since higher velocities were required in order to achieve the same flow rate at a higher pressure difference (smaller opening). The volume-averaged  $DR$  for the non-regulating case POS2-10Pa was only slightly higher (8.87 vs. 5.89 for the regulating case), but it should be kept in mind that the high heating device capacity (almost doubled as compared to the self-regulating case), causes a reduction of  $DR$  by increasing the room temperature.

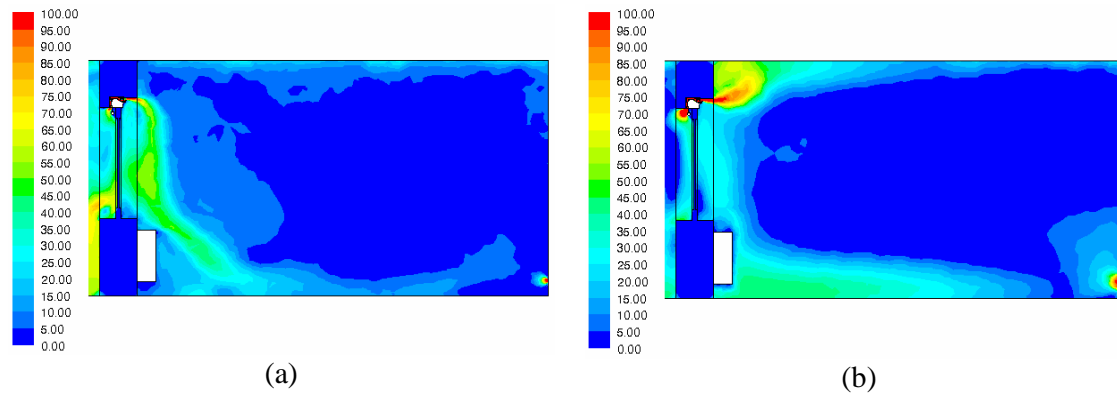


Figure 4: Draught risk [%] for (a) the self-regulating case POS10-10Pa and (b) the non-regulating case POS2-10Pa

## CONCLUSION

CFD was used as a valuable tool for demonstrating the ability of a self-regulating pressure-sensitive air transfer device to achieve a uniform flow rate throughout the normal range of pressure differences for natural ventilation. Besides, CFD proved very useful for studying air distribution and movement in a climate room, and for evaluating effects of the air transfer device on human comfort by assessing draught risk. CFD results demonstrated that self-regulating air transfer devices can decrease the risk on draught compared with non-regulating devices. Besides, mutual effects of air transfer devices and heating devices can be studied.

## REFERENCES

- AIVC (1990). Fundamentals of the multizone air flow model-COMIS. *AIVC Technical Note 29*.
- Dorer, V., Pfeiffer, A. and Weber, A. (2005). Parameters for the design of demand controlled hybrid ventilation systems for residential buildings. *AIVC Technical Note 59*.
- Jones, P.J. and Whittle, G.E. (1992). CFD for building air flow prediction – current status and capabilities. *Building and Environment 27:3*, 321-338.
- Koontz, M.D. and Nagda, N.L. (1991). A multichamber model for assessing consumer inhalation exposure. *Indoor Air 4*, 593-605.
- Nielsen, P.V. (1992). Description of supply openings in numerical models for room air distribution. *ASHRAE Transactions 98:1*
- Sparks, L.E.B.A., Tichenor, B.A., Cang, J. and Guo, Z. (1996). Gass-phase mass transfer model for predicting volatile organic compound (VOC) emission rates from indoor pollutant sources. *Indoor Air 6*, 31-40.